J Exp Biol Advance Online Articles. First posted online on 18 December 2014 as doi:10.1242/jeb.111633
Access the most recent version at http://jeb.biologists.org/lookup/doi/10.1242/jeb.111633

Evidence for a Carotid Body Homolog in the Lizard *Tupinambis merianae*

Michelle N. Reichert, Deidre L. Brink and William K. Milsom

Department of Zoology, University of British Columbia,

Vancouver, British Columbia, V6T 1Z4

Summary

The homolog to the mammalian carotid body has not yet been identified in lizards. Observational studies and evolutionary history provide indirect evidence for the existence of a chemoreceptor population at the first major bifurcation of the common carotid artery in lizards, but a chemoreceptive role for this area has not yet been definitively demonstrated. We explored this possibility by measuring changes in cardiorespiratory variables in response to focal arterial injections of the hypoxia mimic sodium cyanide (NaCN) into the carotid artery of 12 unanesthetized specimens of *Tupinambis merianae*. These injections elicited increases in heart rate (f_H; 101±35% increase) and respiratory rate (f_R; 620±119% increase), but not mean arterial blood pressure (MAP). These responses were eliminated by vagal denervation. Similar responses were elicited by injections of the neurotransmitters acetylcholine (ACh) and serotonin (5-HT) but not norepinephrine. Heart rate and respiratory rate increases in response to NaCN could be blocked or reduced by either the antagonist to ACh (atropine) and/or 5-HT (methysergide). Finally, using immunohistochemistry we demonstrated the presence of putative chemoreceptive cells immuno-positive for the cholinergic cell marker vesicular ACh transporter (VAChT) and 5-HT on internal lattice-like structures at the carotid bifurcation. These results provide evidence for the existence of dispersed chemoreceptor cells at the first carotid bifurcation in the central cardiovascular area in lizards with similar properties to known carotid body homologs, adding to the picture of chemoreceptor evolution in vertebrates.

Key Words: Reptiles, Lizards, tegu, arterial chemoreceptors, oxygen chemoreception, carotid body, ACh, serotonin

Introduction

Chemoreceptors play an important role in monitoring environmental and/or blood gases and regulating ventilation and perfusion in order to maintain metabolic homeostasis under changing conditions. Peripheral chemoreceptive sites in terrestrial vertebrates are believed to be evolutionarily derived from neuroepithelial cells (NECs) associated with the gill arches of fish (Laurent 1984; Milsom and Burleson 2007; Jonz and Nurse 2012). All oxygen chemoreceptors release neurotransmitters when stimulated by hypoxia, hypercapnia or changes in pH. The rate of neurotransmitter release is correlated to the level of hypoxia and acts on secondary afferent neurons. These neurons project to the brainstem where they initiate a reflex arch that changes breathing and heart rate in a way that restores arterial levels of oxygen.

Based on the known homology between the gill arches of fish and the arteries of other vertebrates as well as cell characteristics, NECs of the first gill arch (the third brachial arch) are hypothesized to be the ancestral homologs of the glomus cell chemoreceptors found in mammals. In mammals, the glomus cells or chromaffin cells converge into a collective mass called the carotid body (Gonzalez *et al.* 1994; Peers and Kemp 2001). Homologs to the mammalian carotid body have been found in amphibians (Neil *et al.* 1950; Van Vliet and West 1992; Kusakabe 2002; Jonz and Nurse 2012) and birds (Abdel-Magied and King 1978; Kameda 2002) but a homolog has not yet been identified in reptiles.

There are currently ongoing studies of the carotid body homologs in turtles and snakes (Reyes *et al.*, 2014), but none in lizards or crocodiles. In lizards, observational studies have found small groups of glomus-like cells at the first major bifurcation of the ascending carotid artery (Adams 1953), but evidence to support chemoreceptive ability and homology to the mammalian carotid body has not been presented.

One defining physical characteristic of chemoreceptive cells is the presence of neurochemicals used in the communication between the cells and the synapsing afferent neurons. While almost all known neurochemicals have been found in mammalian glomus cells (Gonzalez *et al.* 1994), the neurochemical makeup of fish, amphibian and avian chemoreceptor cells is more limited. For this study, we tested for cell markers of acetylcholine (ACh) and serotonin (5-HT) based upon their prevalence in the carotid chemoreceptor cells of other taxa.

Catecholamine- and serotonin-containing cells are present in the chemoreceptive regions of fish, amphibians, birds and mammals (Banister *et al.* 1967; Kameda 2002; Burleson *et al.* 2006; Prabhakar 2006; Jonz and Nurse 2012) while ACh is found in some fish and all mammals (Burleson and Milsom 1995; Nurse 2005). Although ACh is not found in the carotid chemoreceptors of all taxa, cholinergic putative chemoreceptor cells were recently found in chelonians (Reyes *et al.*, 2014), leading us to include it in our study. We chose to use the catecholamine norepinephrine in our injection experiments because it is known to stimulate breathing and heart rate in reptiles (Akers and Peiss 1963). We did not expect to elicit a response with this neurotransmitter, however, as there is no evidence of catecholamines in putative carotid chemoreceptors of other reptiles (Reyes *et al.*, 2014).

We sought to test Adams' (1953) hypothesis on the location of carotid chemoreceptive cells in the South American black and white tegu lizard *Tupinambis merianae* and describe the characteristics of the site, should it give rise to chemoreceptive reflexes. We conducted pharmacological studies to examine whether cardiorespiratory responses could be initiated by arterial chemoreceptors at the carotid bifurcation when exposed to chemical hypoxia. We then examined their homology to mammalian glomus cells by studying the neurochemical markers of putative chemoreceptive cells in this area and the reflex responses to arterial injections of agonists and antagonists of these neurochemicals.

Results

Injection Results

NaCN

A 0.25 ml injection of saline, used to control for the physical effects of a bolus injection, resulted in a small increase in heart rate (f_H) that returned to control levels over roughly 2.5 minutes (Figure 1A). The change in f_H in response to an injection of NaCN was significantly larger. Breathing frequency (f_R) also increased rapidly in response to NaCN and remained elevated for over 5 minutes (Figure 1B) while the saline injection resulted in only a transient increase in f_R. There were no statistically significant differences in mean arterial blood pressure (MAP) between the NaCN injection and the saline injection (Figure 1C).

Acetylcholine and Serotonin

Injection of ACh and 5-HT both resulted in significant increases in f_H, compared to the saline injection, lasting 4.5 and 5.5 minutes, respectively (Figures 2A and 3A). In contrast, the increase in f_R in response to ACh and 5-HT was more transient, lasting less than a minute before returning to pre-injection levels (Figures 2B and 3B). Injection of ACh did not cause any significant change in blood pressure (Figure 2C) while bolus 5-HT injection produced a large and significant increase in MAP, which was maintained over 5 minutes (Figure 3C).

Norepinephrine

Injections of norepinephrine resulted in a significant increase in f_H, but due to large variability, this increase was not significantly different than the increase obtained following saline injection (Figure 4A). After a small initial increase, norepinephrine depressed f_R significantly below resting levels (Figure 4B). Figure 4C shows that norepinephrine immediately increased MAP, which continued to rise for 5 minutes.

Neurotransmitter Antagonists

Atropine was injected to block muscarinic ACh receptors in the area of the carotid bifurcation. A secondary injection of ACh (graphs not shown) was used to ensure the injection of atropine had successfully blocked the receptors, which it had. NaCN was then injected to determine the extent to which blocking ACh receptors affected responses to NaCN injection. Both NaCN and ACh alone resulted in similar increases in f_H. Atropine eliminated the f_H response to NaCN (Figure 5A). Injections of NaCN and ACh produced very different changes in f_R (Figure 5B). NaCN caused a prolonged elevation while ACh caused a very short increase in f_R. Injection of atropine resulted in a reduction of the initial increase in f_R and an elimination of the long term elevation seen following the NaCN injection. There were no significant differences in MAP between treatments.

The 5-HT receptor antagonist methysergide reduced the increase in f_H and f_R seen when NaCN alone was injected, although it did not completely eliminate either response (Figure 6A and 6B). 5-HT resulted in a much larger increase in f_H than that produced by NaCN, but did not

increase f_R to the same extent. While 5-HT produced a large increase in MAP, neither NaCN alone nor methysergide + NaCN produced any significant changes in MAP (Figure 6C).

When atropine and methysergide were injected in series, the increases in f_H and f_R normally seen upon injection of NaCN were completely eliminated (Figure 7A and 7B).

Denervation

Due to surgical difficulties, it was not possible to gather f_H and f_R responses before the animals were denervated. It was therefore necessary to compare data from denervated individuals (N=4 for NaCN injection; N=3 for ACh and 5-HT injections) with data from intact individuals (N=6). Unilateral vagal denervation resulted in the complete loss of the f_H and f_R responses to NaCN, ACh and 5-HT injections on that side (Figures 8, 9 and 10).

Anatomy and Immunohistochemistry Results

The external structure of the carotid bifurcation was found to vary both within and between the individuals used in this study (Figure 11). Within each individual, there were size differences between the left and right carotid bifurcation (Figure 11A). Between individuals, there are considerable differences in branching pattern, ranging from simple (Figure 11B) to more complicated (Figure 11C). The internal structure at the carotid bifurcation consists of thin cords of tissue running across the vessel lumen, connected to the vessel wall with folds of tissue. The cords and folds create a lattice-like structure (n> 15 observations, Figure 12).

Using immunohistochemistry, we tested for 5-HT and vesicular ACh transporter (VAChT) in control tissues (adrenal gland and skeletal neuromuscular synapse, respectively) and carotid endothelial cells lining the interior of the carotid bifurcation region. We did not test comprehensively for catecholaminergic cells in the area due to the lack of response to norepinephrine injections. Also, a previous study was unsuccessful in detecting catecholamine-containing cells in the homologous region of red-eared slider turtles (Reyes *et al.*, 2014). Some adrenal gland cells colabelled for two different serotonin primary antibodies, one made in rabbit and one in goat (Figure S1A). Neural processes innervating skeletal muscle labelled positive for VAChT and SV2 (synaptic vessicle marker; Figure S1B). Whole mounts of carotid arteries were used to look for 5-HT and VAChT expression. Endothelial cells on the surface of the internal

lattice were positive for VAChT labelling alone (Figure S2B n=3), 5-HT labelling alone (Figure S2A n=2), and some cells were positive for both (n=3, Figure 13 A and B). The immunopositive cells that labelled for VAChT and 5-HT had oval cell bodies, some with cytoplasmic extensions (Figure S2 and 13). These endothelial cells were on the surface of the internal lattice structures, exposed to the lumen of the vessel (Figure 13 and S Movie 1).

Discussion

Observational studies and evolutionary history have provided indirect evidence for the existence of a cardio-respiratory chemoreceptor population at the first major bifurcation of the common carotid artery in reptiles (Adams 1953; Kardong 2006). Recently, physiological and immunohistological studies in turtles and snakes has provided evidence for the existence of carotid chemoreceptors homologous to mammalian glomus cells (Reyes *et al.* 2013). In snakes putative chemoreceptor populations occur at the carotid bifurcation and at the base of the aortic arch and pulmonary artery while in turtles populations are found in the common carotid artery, aorta and pulmonary artery (Reyes *et al.* 2014, submitted). The present study is the first to characterize putative chemoreceptor populations in lizards at a similar site. The physiological and immunohistochemical data presented in this study support the existence of a carotid body homolog at the first carotid bifurcation of tegu lizards possessing putative chemoreceptive cells with similar characteristics to glomus cells.

Effect of Saline and NaCN Injections on Cardiorespiratory Variables

Injections of saline did not have a significant effect on f_H, f_R or MAP. The slight increase in MAP and the accompanying small increase in f_H most likely reflect transient volume loading and not baroreceptor stimulation. Baroreceptor stimulation should result in a fall in heart rate and thus these data also suggest that baroreceptors are not present at this site, or are not responsive to these small increases. Similar results have been obtained in previous studies in turtles (Berger *et al.* 1980; Berger 1987).

Injections of NaCN produced maximal increases in f_H and f_R of 101±35% and 620±119%, respectively. The small increase in MAP observed was not significantly different from that induced by the saline injections. The hyperventilation was predicted to increase the amount of oxygen moving across the lung epithelia into the blood and the accompanying tachycardia was

expected to increase delivery of the oxygen to the tissues. These increases in f_H and f_R contrast with previous studies on *Tupinambis merianae,* however, which found that reducing inspired P_{O_2} resulted in a slight decrease in f_H and an increase in ventilation exclusively through an increase in tidal volume (V_T) while f_R remained unchanged (Skovgaard and Wang 2004; Skovgaard *et al.* 2005).

The differences between these studies may reflect differences in levels of chemoreceptor stimulation and/or differences in the site of action. The injections of NaCN used in the present study produced a localized, transient stimulus at a single chemoreceptive site. In the study of Skovgaard *et al.* (2005), generalized hypoxia was sustained and would have acted at multiple chemoreceptive sites. Also, due to the design of our experiment, we could only measure changes in f_R and not changes in tidal volume (V_T). The data of Skovgaard and Wang (2004) suggest that we should have seen a large increase in V_T in our experiments and therefore the increase in ventilation was most likely much greater than our data suggest. This is supported by subjective observations of increased impedance after each NaCN injection.

The Effects of Neurochemicals on Cardiorespiratory Variables

Many neurochemicals are involved in chemoreception across vertebrate taxa (reviewed in Milsom and Burleson 2007). We focused on testing for the presence and physiological effect of ACh, 5-HT and catecholamines based on the prevalence of these neurochemicals in other taxons. Immunohistochemistry revealed serotonergic and cholinergic cells in the area of the carotid bifurcation. Although most of the cells in the carotid lattice were positive for both 5-HT and VAChT, some cells expressed only 5-HT or VAChT immunoreactivity. Both the singly labeled and the colabeled cells were dispersed as well as clustered on the cross-cords of the internal lattice. Additionally, cursory inspection showed VAChT+/5-HT+ cells proximal and distal to the internal carotid labyrinth albeit at lower density. Thus, the internal carotid lattice, which effectively expands the lumen surface area of the carotid artery, is an area where candidate respiratory gas sensing cells are aggregated.

The VAChT+/ 5-HT+ cells we found were similar to respiratory gas sensing cells in mammals, as multiple transmitter expression also occurs in mammalian carotid body sensory cells (Zhang and Nurse 2004; Piscurik and Nurse 2012) and in mammalian aortic body cells

(Dvorakova & Kummer, 2005; Piscurik and Nurse 2012). Establishing the gas sensing function of the cells described here requires functional tests at the cellular and neural circuit level, for example using electrophysiology. Although direct testing for respiratory gas sensitivity in the VAChT+/5-HT+ cells was beyond the scope of this study, the cells found are good candidates for respiratory gas sensing based on their location and their similarity to known gas sensing cells in other animals. The neurotransmitter profile of the putative chemoreceptor cells also correlates well with the physiology and pharmacology data.

Cardiovascular Variables

Injections of all three neurochemicals resulted in an increase in f_H, but this increase was significantly higher than the saline injection values only for injections of ACh and 5-HT (Figures 2A, 3A and 4A). Injections of 5-HT and norepinephrine also resulted in significant increases in MAP (Figures 2C, 3C and 4C).

Injection of atropine blocked the effect of NaCN on f_H (Figure 5A). This suggests that muscarinic ACh receptors are involved in hypoxia chemoreception and, by extension, that ACh is an important neurotransmitter in the initiation of the cardiovascular response to hypoxemia. These results are supported by previous studies on turtles and rattlesnakes, which found that injection of atropine eliminated the tachycardia normally seen during hypoxia exposure (Comeau and Hicks 1994; Skovgaard *et al.* 2005).

Injection of methysergide also blocked the effect of NaCN on f_H (Figure 6A), suggesting that 5-HT_2 receptors are also involved in hypoxia chemoreception and that 5-HT is also an important neurotransmitter in the initiation of the hypoxic cardiac response.

Norepinephrine injections also produced an increase in f_H but this was not significantly different than the increase caused by the injection of saline alone. The response was highly variable and we hypothesize that the increase in f_H may not have been a direct effect of norepinephrine acting on chemoreceptors in this region but an indirect effect of its action elsewhere.

Because blood pressure was not appreciably changed upon injection of NaCN, we assumed that any significant changes in MAP upon injection of ACh, 5-HT or norepinephrine

would reflect a response due to interactions with the smooth muscle of the vessel wall and not arterial chemoreceptors. We predicted that we would see an increase in MAP upon injection of 5-HT and norepinephrine because both of these neurotransmitters are known to cause vasoconstriction (Vanhoutte 1974; Kahn *et al.* 1992) while ACh does not (Kirby and Burnstock 1969; Vanhoutte 1974). Our data match these predictions. Neither atropine nor methysergide significantly affected the response of MAP to the injection of NaCN.

Respiratory Variables

Injections of ACh and 5-HT resulted in only a transient increase in f_R (Figures 2B and 3B) while NaCN injections produced a larger and much longer lasting response. The transient nature of the increase in f_R in response to ACh and 5-HT injections could reflect rapid metabolism of ACh and 5-HT at the chemoreceptor site while the longer response to NaCN could reflect slower metabolism of this exogenous compound. In contrast, injection of norepinephrine appeared to depress f_R (Figure 4B).

After the injection of atropine or methysergide to block ACh and 5-HT receptors respectively, there was both a reduction in the initial breathing response and a total abolition of the prolonged breathing response that normally occurred upon NaCN injection. This suggests that both ACh and 5-HT are important in the initiation of the hypoxic ventilator response (HVR). In mammals, methysergide also abolishes the HVR (Millhorn *et al.* 1980) but atropine has been found to have no effect on ventilatory responses to NaCN (de Burgh Daly *et al.* 1978).

Effects of Denervation

After denervation, the injection of NaCN, ACh and 5-HT no longer resulted in significant increases in f_H and f_R (Figures 8, 9 and 10). Transection of the vagus nerve in our study was performed high in the neck, at the site of cannulation, and would have eliminated sensory feedback from sites other than just the carotid bifurcation. While this does not allow us to rule out possible effects of our injections at other arterial chemoreceptive sites, it does allow us to rule out any central effects or direct effects on the heart.

General Conclusions

Possible Neurochemical Relationships

Based on the physiological and immunohistological data collected, we conclude that both ACh and 5-HT, but not norepinephrine, are involved in the production of cardio-respiratory reflexes arising from stimulation by NaCN in the vicinity of the first bifurcation of the common carotid artery in the tegu lizard. We found strong immunohistochemical evidence for colabeling of many cells in the lining of the carotid vessel with 5-HT and VAChT while some cells where positive for either marker alone. The VAChT+/5-HT+ cells were dispersed and clustered on the surface of an extensive lattice-like internal structure. The presence of serotonin and a cholinergic marker in many of the same cells suggests that they may be cotransmitters. That antagonists to either neurotransmitter alone blocked the cardio-respiratory responses to NaCN also suggests that ACh and 5-HT are cotransmitters that interact with the downstream sensory network. The nature of this interaction remains to be worked out.

While our data strongly support the presence of chemoreceptor cells at the carotid bifurcation of tegus, all evidence we gathered in this study is indirect. In order to provide direct evidence of the chemoreceptive function of these cells, nerve recordings should be taken from the fibres synapsing with the putative chemoreceptive cells. Such recordings should be taken close to the proposed site of chemoreception. Due to the nature of our surgeries, we were forced to cut the vagus nerve high in the neck, therefore potentially influencing multiple chemoreceptive sites and not solely the site of interest. Also, the design of this experiment makes it uncertain if the agonists and antagonists for 5-HT and ACh were acting directly on the putative chemoreceptors in the region of the carotid bifurcation. However, the presence of cells containing these neurotransmitters, the fact that the area is innervated, and the elimination of responses to these drugs following denervation of the vagus are all highly suggestive that the effects of these drugs are direct.

Evolution of Carotid Chemoreception

Similar to all other semi-terrestrial and terrestrial vertebrates (i.e. amphibians, birds and mammals) (Heistad and Abboud 1980; Faraci 1986; Kruhoffer *et al.* 1987; van Klaveren and Demedts 1998; Andersen *et al.* 2003), stimulation of putative carotid artery chemoreceptors in lizards produced an increase in f_H and f_R while keeping MAP constant. The physical association of chemoreceptive cells in the carotid artery of the tegu, however, differed from the general pattern seen in most other terrestrial taxa. The carotid chemoreceptors of amphibians and

mammals are concentrated into highly vascularized structures (the carotid labyrinth and carotid body respectively) (Gonzalez *et al.* 1994; Kameda 2002; Kusakabe 2002). In contrast, the chemoreceptive site in the tegu is best described as a modified artery with a lattice-like structure composed of cords of tissue crisscrossing the vessel lumen, within which the putative chemoreceptor cells are diffusely distributed. This site is not high in the neck but is located in the central vasculature at the site of the first bifurcation of the common carotid artery. The primary neurotransmitters involved in the reflexes arising from this site are ACh and 5-HT. This is consistent with recent research in turtles in which ACh and 5-HT were also shown to be the primary neurotransmitters associated with oxygen chemoreception in the aorta and carotid and pulmonary arteries although in turtles they are not colocalized (Reyes *et al.*, 2014). This is similar, however, to the situation seen in mammals where multiple transmitters co-label to a common cell type. Despite any differences in the physical characteristics and distribution of the chemoreceptive cells and organs, it appears that the function of the cells is highly conserved.

Materials and Methods

Experimental Animals

This study was conducted at two different locations. Experiments were performed on six tegus (weighing 2.82 ± 0.68 kg) at the University of British Columbia in the summer of 2012 and six additional tegus (weighing 2.50 ± 0.84 kg) at the Jacarezario, UNESP Bela Vista Campus, Rio Claro, SP, Brazil. All tegus were Brazil-bred, raised in captivity and housed in groups in large enclosures within an animal care facility at each location. The holding and experimental procedures followed the Canadian Council on Animal Care guidelines and were approved by the University of British Columbia Animal Care Committee (animal care certificate number A12-0068).

Surgical Procedures

In all animals, drug injections were made and blood pressure was measured via a cannula inserted into the left or right internal carotid artery, with its tip sitting at the first major bifurcation of the common carotid artery on that side. For the surgical insertion of the cannula, the lizards were anaesthetized with Isoflurane (Abbott Animal Health) and artificially ventilated at 12 breaths/min (25 ml/breath) using a Harvard Apparatus Respirator and medical grade

compressed air (Praxair). The air was humidified and passed through an Isoflurane vaporizer (Drager, Lubeck, Germany) set at 1-2% of inhaled air throughout the surgery. To insert the cannula, a 4-6 cm incision was made approximately 3 cm behind the left ear of the animal, the internal carotid artery was then isolated and cannulated with polyethylene tubing (Clay Adams Brand, size PE90). In three individuals, the nerve believed to be synapsing with the carotid bifurcation was isolated in the same region that the cannula had been inserted and cut before the incision was closed. Before the cannula was closed, approximately 5ml of reptile saline (136.89mM NaCl, 2.68mM KCl, 1.80mM $CaCl_2$, 1.58mM $MgCl_2$, 11.90mM $NaHCO_3$, 0.33mM NaH_2PO_4, and 5.55mM glucose) was injected to combat dehydration.

Electrical leads were implanted subcutaneously during surgery to measure heart rate and breathing frequency. After the cannula was inserted, five additional 1cm incisions were made for the insertion of the electrical leads. One electrical lead for breathing frequency was inserted lateral to each lung. The remaining three electrical leads (for heart rate) were inserted subcutaneously: one on the ventro-lateral side of the body just above the heart, one on the opposite ventro-lateral side of the body just below the heart and one on the ventro-lateral side of the body 2-3 cm superior to the left lower limb. Each incision was closed with one suture. The wires from the electrical leads and the cannula were then coiled up and wrapped tightly against the lizard's body using athletic wrap (Nexcare, 3M Coban Self-Adherent Wrap).

The lizards were kept artificially ventilated without Isoflurane until they regained consciousness and started breathing on their own (this took 2 to 8+ hours depending on the individual). Occasionally a heating blanket (set on low) would be wrapped around the lizard to increase its metabolic rate and thus decrease the time required for it to regain consciousness. The analgesic meloxicam (dose 0.2 mg/kg) was injected IM before the lizard regained consciousness. The lizard was then placed in a small container with water and allowed to recover overnight.

Measurements of Blood Pressure, Heart Rate and Breathing Frequency

During the experiment, injections were made through the cannula and blood pressure was measured via the cannula using a pressure transducer (Utah Medical Products Inc., Midvale, Utah, USA), which was calibrated daily using a barometer. Heart rate was measured using a Grass Model 79E EKG and polygraph data recording system (Grass Instrument Co., Warwick,

Rhode Island, USA) and breathing frequency was measured using an impedance converter (UFI, model 2991, Morro Bay, California, USA). Tidal volume could not be measured via the impedance converter due to the movement of the animals, which created the need for constant readjustment of the impedance balance.

Injections

A series of chemicals and drugs were injected into the internal carotid artery via the cannula. All animals were subjected to bolus injections of 0.25 ml of 1.0 mg/ml sodium cyanide, 0.1 ml of 10 mg/ml acetylcholine chloride, 0.25 ml of 2.5 mg/ml serotonin hydrochloride and 0.25 ml of 1.0 mg/ml DL-norepinephrine hydrochloride. The drug antagonists methysergide maleate (blocker of 5-HT_2 receptors) and atropine (blocker of muscarinic ACh receptors) were also injected (0.2 ml of 0.1 mg/ml methylsergide maleate and 0.2 ml of 0.30 mg/ml atropine). All drugs were purchased from Sigma-Aldrich. Concentrations considered safe for injection were determined from literature values (Kirby and Burnstock 1969; Hohnke 1975; Skovgaard et al. 2005).

Experimental Protocol

After the animal had recovered from surgery, the electrical leads were unwrapped and connected to their respective measuring instruments. Animals were then left undisturbed for several hours. Measurements in resting animals were taken for 10 minutes before the first injection. After 10 minutes, NaCN was injected via the cannula, followed by approximately 1 ml of saline in order to ensure the drug cleared the catheter and reached the artery. The bolus was injected at a gradual rate to avoid any injection artefact. During this time, blood pressure could not be measured due to the cannula being used for injection. After each injection, at least 10 minutes was allowed before the next injection to ensure that a new resting state had been reached. If any variable was still altered significantly from starting values after 10 minutes, additional time was allowed before the next injection. Following NaCN, neurotransmitter agonists ACh, 5-HT and norepinephrine were injected in random order. A bolus of saline was injected as a control between injections of each drug.

After NaCN and all neurotransmitter agonists were injected, one of the two neurotransmitter antagonists was injected. Ten minutes after the injection of the antagonist, the

complimentary agonist was injected to ensure the antagonist had successfully blocked the receptors. After 10 minutes had elapsed, NaCN was once again injected and the response recorded. The animal was then allowed to recover overnight before the next antagonist was injected to ensure that the previous antagonist was completely metabolized. In five animals, both atropine and methysergide were injected in series, followed by NaCN.

After all the necessary injections were carried out, the animals were euthanized via an overdose of urethane and the carotid bifurcation that was not cannulated was dissected out for immunohistochemistry. In denervated individuals, the cut nerve was isolated and traced back to the carotid bifurcation to ensure the correct nerve had been sectioned.

Data Collection, Analysis and Statistics

All signals from the pressure transducer, EKG and impedance converter were collected on a computer at a sample rate of 250 Hz using Windaq acquisition software (DATAQ Instruments Inc., Akron, Ohio, USA). Blood pressure data was collected as systolic (SBP) and diastolic (DBP) blood pressures, then converted to mean arterial blood pressure (MAP) via equation (1).

$$MAP = DBP + \frac{1}{3(SBP - DBP)} \quad (1)$$

Raw data were analyzed in 30 second bins from 1.5 minutes prior to an injection to 5.5 minutes following the injection. The 1.5 minutes of resting recordings were averaged and set to zero. All data are shown as absolute differences and are represented in figures as means ± 1 standard error of the mean (S.E.M).

Data were statistically analyzed using SigmaStat version 3.5 (Systat Software Inc., San Jose, California, USA). A two-way repeated measures ANOVA was used to determine significant differences (defined as $P<0.05$) between treatments and over time within a treatment. If significant differences were detected by the ANOVA, a Holm-Sidak *post-hoc* test was used to determine where the differences occurred. Non-normal data were natural log transformed.

Immunohistochemistry

Immunohistochemistry was performed on tissue harvested from euthanized animals. We used conventional cryosectioning techniques to check for antibody reactivity in tissues likely to express 5-HT (spinal cord) and ACh (the neuromuscular junction of skeletal muscle). For cryosectioning, tegu tissue samples were placed in 4% paraformaldehyde (PFA)/reptile ringer buffered to pH 7.45 (PFA: Electron Microscopy Sciences) and stored in fixative for 3 weeks then rinsed 3 x 15 ml of ice cold reptile ringer. The tissue blocks were transferred to cryoprotectant (sucrose 300 g; PVP-40 10 g; 500 ml PBS; and 300 ml ethylene glycol, with double distilled H_2O added for a 1 liter final volume) and sunk in 3 x 15 ml cryoprotectant at 4 ^{o} C. Cryoprotected tissue was embedded in Tissue Tek (Electron Microscopy Sciences) and rapidly frozen to -20 ^{o} C. Following freezing, embedded tissue was sectioned in 12µm thick sections which were placed on Permafrost slides (VWR Canada). Slide mounted tissue was incubated with 10% normal donkey serum (Cedarlane, Canada) for 1 hour in a humid box. Slides were then incubated for 24 hours at room temperature in primary antibodies at a volume concentration of 1:100, 1:200 or 1:400 in a solution of 0.02% triton X (Sigma). Primary antibodies were rinsed off tissue sections with three rinses of PBS ringer before the tissue sections were incubated with fluorescently tagged secondary antibodies at a concentration of 1:100 for 12 hours in a moist, dark chamber. The tissue sections were then rinsed 3 more times in PBS ringer, mounted in Vectashield with DAPI (Vector Labs) and coverslipped with #1.5 coverslips. Prepared slides were stored in dark boxes at 4 ^{o} C (for antibody details see Table 1 and 2).

To demonstrate the specificity of the anti-VAChT and anti-5-HT primary antibodies, we labelled frozen sections tegu skeletal muscle (two animals, three samples per animal) and adrenal cortex (two animals, three samples per animal) with the respective primary at dilutions of 1:100, 1:200 and 1:400. Both 5-HT primary antibodies labelled the same cells in adrenal gland (Figure S1 A). Both SV2 (a synaptic vesicle antibody) and VAChT colabeled the same features at the neuromuscular synapse (Figure S1). We used whole mounts of carotid arteries (Piscuric and Nurse 2012) to demonstrate the cellular morphology and distribution of 5-HT+ and VAChT+ (cholinergic) cells within the lumen of the carotid artery. For the carotid vessel whole mounts, the common carotid arteries and all branches extending approximately 3-5 cm from the bifurcation were dissected out of the body. Excessive connective tissue was dissected away in ice-cold reptile saline (see above). The carotid arteries were placed in ice-cold 4% paraformaldehyde (Electron Microscopy Sciences) in reptile PBS buffered to a pH of 7.45 and

stored in fixative for three weeks at 4º C. Post-fixation, the blood vessels were rinsed three times with ice cold PBS ringer. Carotid vessel whole mounts were made by pinning the vessels out under slight tension onto a small Sylgard (Dow Corning) floored tray, using stainless steel 000 insect pins (Austerlitz). Each vessel was cut open longitudinally with the luminal face exposed, with care taken not to damage the internal vascular structures. The opened vessels were then rinsed three times with cold PBS ringer, then put in a permeablizing solution (.02% Triton X, Sigma Aldrich, in reptile PBS ringer pH 7.45) containing rabbit anti-VAChT (concentration 1:100) and goat anti-serotonin (concentration 1:100) primary antibodies blocked with 5% normal donkey serum (Cedarlane, Canada) for 48 hours at 27 º C. Post-incubation, the primary antibody solution was rinsed off with ice cold reptile PBS. In double labelled carotid tissue, we used the goat anti-5-HT antibody together with the VAChT probe made in rabbit to ensure separate detection of each antibody. Secondary fluorescently tagged antibodies (concentrations 1:100) were applied in two separate steps to control for PFA fluorescence (due to a long storage time in fixative) and green fluorescent emission into the "red" channel arising from broad 2-photon excitation responses evoked with the excitation beam set to 780 (Werkmeister et al. 2007). Emissions were collected into two separate photomultiplier channels filtered to separate green and red emissions. To show VAChT labelling in isolation, the first round of secondary labelling was done for 24 hours at 27 º C using a donkey anti-rabbit Alexa 594 conjugate in .02% triton X in reptile ringer, followed by 3 ringer rinses. The whole mounts were put in filtered ringer and covered by # 1.5 coverslips sealed in place with paraffin wax. Testing for colabeling of serotonin with VAChT+ cells was done with a second round of donkey anti-goat Alexa 488 for 24 hours at 27 º C, rinsed, and both 594 and 488 labelled antigens imaged with 2-photon excitation in 3 whole mounts. Data on separately labelled VAChT+ cells and 5-HT positive cells in the carotid lattice were collected with a spinning disk microscope (Figure S2 A and B). Information on antibodies and imaging are presented in Table 1 and 2 respectively. Lastly, we repeated the secondary antibody labeling without primary labeling to carotid whole mounts to assess non-specific secondary fluorescence, which was negligible (one preparation, data not shown).

Microscopy

To image whole mounted tissue, we used an Olympus (Japan) XZ10 steromicroscope equipped with a digital camera to photograph the internal structure of an interior carotid lattice

whole mount, using Olympus Cellsens software. Cryosectioned data and some control whole mounts were gathered with a Perkin Elmer Ultraview VoX Spinning Disk Confocal microscope (Leica/Perkin Elmer), using a 20 x multi-immersion objective (.75 NA), correction set for glycerol or water, and Volocity software for image capture. To image the thick, light scattering whole mount tissue, we used an Olympus FV1000 microscope with a 25 X long-working length objective (NA 1.05). A Mai Tai Deep See laser (Olympus) was used for pulsed laser excitation; with Olympus acquisition software. Data were gathered at a scan rate of 4 microseconds/pixel with 1 micron spacing between optical sections. We used a stringent red emission filter to ensure that high intensity green emission did not cross-talk with the PMT red channel (Werkmeister et al 2007), which effectively reduced 594 signal collection by about 40%. Image data were made into figures using NIH image J (Schneider et al. 2012) and Photoshop 7.0 (Adobe). Brightness and contrast were adjust using linear scales only.

Acknowledgements: This research was supported by the NSERC of Canada. We are greatly indebted to the assistance of the UBC Botany/Zoology Bioimaging Facility and to Denis Andreade, Augusto Abe, Ze Carvalho and Cleo Leite for logistic and intellectual support.

Funding: This research was supported by the Natural Science and Engineering Research Council of Canada [grant 150-11].

References

Abdel-Magied, E.M. and King, A.S. (1978). The topographical anatomy and blood supply of the carotid body region of the domestic fowl. *J. Anat.* **126**, 535-546.

Adams, W.E. (1953). The carotid arch in lizards with particular reference to the origin of the internal carotid artery. *J. Morphol.* **92**, 115-155.

Akers, T. K., and Peiss, C.N. (1963). Comparative study of effect of epinephrine and norepinephrine on cardiovascular system of turtle, alligator, chicken and opossum. *Exp. Biol. and Med.* **112**, 396-399.

Andersen, J.B., Hedrick, M.S. and Wang, T. (2003). Cardiovascular responses to hypoxia and anaemia in the toad *Bufo marinus*. *J. Exp. Biol.* **206**, 857-865.

Banister, R.J., Portig, P.J. and Vogt, M. (1967). The content and localization of catecholamines in the carotid labyrinths and aortic arches of *Rana temporaria. J. Physiol.* **192**, 529-535.

Berger, P.J., Evans, B.K. and Smith, D.G. (1980). Localization of baroreceptors and gain of the baroreceptor-heart rate reflex in the lizard *Trachydosaurus rugosus*. *J. Exp. Biol.* **86**, 197-209.

Berger, P.J. (1987). The reptilian baroreceptor and its role in cardiovascular control. *Am. Zool.* **27**, 111-120.

Burleson, M.L. (2009). Sensory innervation of the gills: O_2-sensitive chemoreceptors and mechanoreceptors. *Acta Histochem.* **111**, 196-206.

Burleson, M.L., Mercer, S.E. and Wilk-Blaszczak, M.A. (2006). Isolation and characterization of putative O_2 chemoreceptor cells from the gills of channel catfish (*Ictalurus punctatus*). *Brain Res.* **1092**, 100-107.

Burleson, M.L. and Milsom, W.K. (1995). Cardio-ventilatory control in rainbow trout: I. Pharmacology of branchial, oxygen-sensitive chemoreceptors. *Respir. Physiol.* **100**, 231-238.

Comeau, S.G. and Hicks, J.W. (1994). Regulation of central vascular blood flow in the turtle. *Am. J. Physiol.: Regul., Integr. Comp. Physiol.* **267**, 569-578.

Coolidge, E.H., Ciuhandu, C.S. and Milsom, W.K. (2008). A comparative analysis of putative oxygen-sensing cells in the fish gill. *J. Exp. Biol.* **211**, 1231-1242.

de Burgh Daly, M., Korner, P.I., Angell-James, J.E. and Oliver, J.A. (1978). Cardiovascular and respiratory effects of carotid body stimulation in the monkey. *Clin. Exp. Pharmacol. Physiol.* **5**, 511-524.

Dupre, R., Hicks, J.W. and Wood, S.C. (1989). Effect of temperature on chemical control of ventilation in Mexican black iguanas. *Am. J. Physiol.* **257**, R1258-R1263.

Dvorakova MC, and Kummer, W. (2005). Immunohistochemical evidence for species-specific coexistence of catecholamines, serotonin, acetylcholine and nitric oxide in glomus cells of rat and guinea pig aortic bodies. *Ann. Anat.* **187**, 323–331.

Faraci, F.M. (1986). Circulation during hypoxia in birds. *Comp. Biochem. Physiol.* **85A**, 613-620.

Gargaglioni, L.H. and Milsom, W.K. (2007). Control of breathing in anuran amphibians. *Comp. Biochem. Physiol.* **147**, 665-684.

Gonzalez, C., Almaraz, L., Obeso, A. and Rigual, R. (1994). Carotid body chemoreceptors: from natural stimuli to sensory discharges. *Physiol. Rev.***74**, 829-898.

Heistad, D.D. and Abboud, F.M. (1980). Dickinson W. Richards Lecture: Circulatory adjustments to hypoxia. *Circulation* **61**, 463-470.

Hoar, W.S. and Hickman, C.P. (1975) A Companion for General and Comparative Physiology. Prentice Hall.

Hohnke, L.A. (1975). Regulation of arterial blood pressure in the common green iguana. *Am. J. Physiol.* **228**, 386-391.

Jonz, M.G., and Nurse, C.A. (2012). Peripheral chemoreceptors in air-versus water-breathers. In *Arterial Chemoreception* (pp. 19-27). Springer Netherlands.

Kahn, A.M., Bishara, M., Cragoe Jr., E.J., Allen, J.C., Seidel, C.L., Navran, S.S., O'Neil, R.G., McCarty, N.A., and Shelat, H. (1992). Effects of serotonin on intracellular pH and contraction in vascular smooth muscle. *Circ. Res.* **71**, 1294-1304.

Kameda, Y. (2002). Carotid body and glomus cells distributed in the wall of the common carotid artery in the bird. *Microsc. Res. Tech.* **59**, 196-206.

Kardone, K.V. (2006). Vertebrates: Comparative anatomy, function, evolution. McGraw-Hill Higher Education, 4th edition, Boston, USA, pp 455-461.

Kirby, S. and Burnstock, G. (1969). Pharmacological studies of the cardiovascular system in the anaesthetized sleepy lizard (*Tiliqua rugosa*) and toad (*Bufo marinus*). *Comp. Biochem. Physiol.* **28**, 321-331.

Kusakabe, T. (2002). Carotid labyrinth of amphibians. *Microsc. Res. Tech.* **59**, 207-226.

Laurent, P. (1984). Gill internal morphology. *Fish Physiol.* **10**, 73-183.

Millhorn, D.E., Eldridge, F.L. and Waldrop, T.G. (1980). Prolonged stimulation of respiration by endogenous central serotonin. *Respir. Physiol.* **42**, 171-188.

Milsom, W.K. and Burleson, M.L. (2007). Peripheral arterial chemoreceptors and the evolution of the carotid body. *Respir. Physiol. Neurobiol.* **157**, 4-11.

Neil, E., Strom, L. and Zotterman, Y. (1950). Action potential studies of afferent fibres in the IXth and Xth cranial nerve of the frog. *Acta Physiol. Scand.* **20**, 338-350.

Nurse, C.A. (2005). Neurotransmission and neuromodulation in the chemosensory carotid body. *Auton. Neurosc.* **120**, 1-9.

Peers, C. and Kemp, P.J. (2001). Acute oxygen sensing: diverse but convergent mechanisms in airway and arterial chemoreceptors. *Respir. Res.* **2**, 145-149.

Prabhakar, N.R. (2006). O_2 sensing at the mammalian carotid body: why multiple O_2 sensors and multiple transmitters? *Exp. Physiol.* **91**, 17-23.

Reyes, C., D. Brink and Milsom, W.K. (2014). Distribution and innervation of peripheral arterial chemoreceptors in the red-eared slider (*Trachemys scripta elegans*). *J. Comp. Neurol.* Submitted.

Schneider, C.A., Rasband, W.S., Eliceiri, K.W. (2012) NIH Image to ImageJ: 25 years of image analysis. *Nature Methods* **9**, 671-675.

Skovgaard, N., Abe, A.S., Andrade, D.V. and Wang, T. (2005). Hypoxic pulmonary vasoconstriction in reptiles: a comparative study of four species with different lung structures and pulmonary blood pressures. *Am. J. Physiol.: Regul. Integr. Comp. Physiol.* **289**, R1280-R1288.

Skovgaard, N. and Wang, T. (2004). Cost of ventilation and effect of digestive state on the ventilatory response of the tegu lizard. *Respir. Physiol. Neurobiol.* **141**, 85-97.

Vanhoutte, P.M. (1974). Inhibition by acetylcholine of adrenergic neurotransmission in vascular smooth muscle. *Circu. Res.* **34**, 317-326.

van Klaveren, R.J. and Demedts, M. (1998). Determinants of the hypercapnic and hypoxic response in normal man. *Respir. Physiol.* **113**, 157-165.

Van Vliet, B.N. and West, N.H. (1992). Functional characteristics of arterial chemoreceptors in an amphibian (*Bufo marinus*). *Respir. Physiol.* **88**, 113-127.

Werkmeister, E., Kerdjoudj, H., Marchal, L., Stoltz, J,F., and Dumas, D. (2007) Multiphoton microscopy for blood vessel imaging: new non-invasive tools (Spectral, SHG, FLIM). *Clin. Hemorheol. Microcirc.* **37**,77-88.

Zhang, M. and Nurse, C.A. (2004). CO2/pH chemosensory signaling in co-cultures of rat carotid body receptors and petrosal neurons: role of ATP and ACh. *J. Neurophysiol.* **92**, 3433–3445.

Figures

Table 1. **Primary antibodies used to immunolabel serotonin (5-HT), vesicular ACh transporter (VAChT), and synaptic vesicles (SV2).**

Table 2. Secondary antibodies used to immunolabel 5-HT, VAChT, and SV2.

Figure 1. **Cardio-respiratory changes in response to injection of NaCN.** The effect of a NaCN injection (red; N=6) on changes in (A) f_H, (B) f_R and (C) MAP over 5.5 minutes. A saline injection (white; N=6) was used as a control on the same animals. Significant differences from pre-injection values (for NaCN) are denoted by + and differences between NaCN and saline injections are denoted by *.

Figure 2. **Cardio-respiratory changes in response to injection of ACh.** The effect of an ACh injection (dark blue; N=6) on changes in (A) f_H, (B) f_R and (C) MAP over 5.5 minutes. A saline injection (white; N=6) was used as a control on the same animals. Significant differences from pre-injection values (for ACh) are denoted by + and differences between ACh and control injections are denoted by *.

Figure 3. **Cardio-respiratory changes in response to injection of 5-HT.** The effect of a 5-HT injection (blue; N=6) on changes in (A) f_H, (B) f_R and (C) MAP over 5.5 minutes. A saline injection (white; N=6) was used as a control on the same animals. Significant differences from pre-injection values (for 5-HT) are denoted by + and differences between 5-HT and control injections are denoted by *.

Figure 4. **Cardio-respiratory changes in response to injection of norepinephrine.** The effect of a norepinephrine injection (green; N=6) on changes in (A) f_H, (B) f_R and (C) MAP over 5.5 minutes. A saline injection (white; N=6) was used as a control on the same animals. Significant differences from pre-injection values (for norepinephrine) are denoted by + and differences between norepinephrine and saline injections are denoted by *.

Figure 5. C**ardio-respiratory changes in response to injection of NaCN following atropine injection.** The effects of a NaCN injection before and after an injection of atropine (before atropine: red; after atropine: yellow; N=6 for both) and an injection of ACh (dark blue; N=6) on changes in (A) f_H, (B) f_R and (C) MAP over 5.5 minutes. + denotes significant differences between NaCN and atropine+NaCN values, * denotes significant differences between ACh and atropine+NaCN values and ^ denotes significant differences between NaCN and ACh values.

Figure 6. **Cardio-respiratory changes in response to injection of NaCN following methysergide injection.** Comparison between the effects of a NaCN injection before and after an injection of methysergide (before methysergide: red; after methysergide: purple; N=6 for both) and a 5-HT injection (blue; N=6) on changes in (A) f_H, (B) f_R and (C) MAP over 5.5 minutes. + denotes significant differences between NaCN and methysergide+NaCN values, *

denotes significant differences between 5-HT and methysergide+NaCN values and ^ denotes significant differences between NaCN and 5-HT values.

Figure 7. C**ardio-respiratory changes in response to injection of NaCN following both atropine and methysergide injections.** Comparison between the effects of a NaCN injection before and after an injection of methysergide and atropine together (before antagonists: red; after antagonists: light blue; N=5 for both) on changes in (A) f_H, and (B) f_R. * denotes significant differences between the injections.

Figure 8. **The effect of denervation on cardio-respiratory changes in response to injection of NaCN.** The effect an injection of NaCN before (red; N=6) and after (black; N=4) denervation of the nerve supplying the carotid bifurcation on changes in (A) f_H and (B) f_R over 5.5 minutes.

Figure 9. The effect of denervation on cardio-respiratory changes in response to injection of ACh. The effect of an injection of ACh before (dark blue; N=6) and after (black; N=3) denervation of the nerve supplying the carotid bifurcation on changes in (A) f_H and (B) f_R over 5.5 minutes.

Figure 10. The effect of denervation on cardio-respiratory changes in response to injection of 5-HT. The effect of an injection of 5-HT before (blue; N=6) and after (black; N=3) denervation of the nerve supplying the carotid bifurcation on changes in (A) f_H and (B) f_R over 5.5 minutes.

Figure 11. The external anatomy of the tegu carotid artery varies both within and between individuals. The size of the carotid arteries can vary within an individual between the left and right sides (A). The branching pattern at the area of bifurcation can vary between animals, ranging from simple (B) to complex (C). Arrows indicate the area of the bifurcation.

Figure 12. **The interior surface area of the tegu carotid artery is expanded by a lattice- like array of tissue cords.** A brightfield image (12 x magnification) of the interior of the carotid artery shows folds and cords of tissue of different thicknesses (arrows). The artery distal to the heart is oriented towards the upper left of the image. Scale bar = 500 microns.

Figure 13. **Serotonin and VAChT colabelled endothelial cells on the surface of the carotid lattice cords.** A) The surface of a lattice cord shown in a 2-D compression of a 3-D image 164 microns thick (for 3-D image see: S Movie 1). VAChT+ (magenta) and 5 HT+ (green) labeled cells are dispersed and clustered on the lumenal surface of the carotid lattice. Colabelled cells appear white. B) A 2.14 X magnification of the boxed region in (A) shows oval cells, with extensions (arrow), colabelled for 5 HT and VAChT. Cell nuclei are unstained. Scale bar: 50 microns.

Supplemental Figures

Figure S1. Cells on the inner surface of the carotid artery "lattice" are immunopositive for 5-HT and VAChT. Two different whole mounted carotid lattices were independently labelled and imaged at the place where cross-cords attach to the blood vessel wall. A) Rabbit anti-serotonin labelled cells (red) lined the inner surface of the carotid lattice. The cells were oval, occasionally had extensions (arrowheads), and round nuclei (DAPI labeling, blue). B) VAChT labelled similar cells (green, arrowheads). Nuclei are unlabelled. Both images are 2- D compressions of 3- D image stacks approx. 40 microns thick. Scale bars: 25 microns.

Figure S2. Antibody labelling patterns for 5-HT (adrenal gland) and VAChT (skeletal muscle). A) Cryosectioned tegu adrenal gland cells co-label for two different anti-serotonin antibodies: rabbit anti- 5-HT (green) and goat anti- 5-HT (red) (arrowheads). DAPI labeled the cell nuclei (blue). Tissue section: 12 microns thick. Scale bar: 50 microns. B) The neuromuscular synaptic region of tegu skeletal muscle labels for VAChT (green) and SV2 (red). Axonal branches terminate on a polynucleated (DAPI, blue) skeletal muscle cell (arrowheads). The skeletal muscle cell showed light scatter in the red channel. Tissue section: 25 microns thick. Scale bar: 50 microns.

S Movie 1. 5-HT and VAChT labelled endothelial cells shown in 3-dimensional projection of the luminal surface of a carotid lattice cord (2- D: Figure 13). The projection rotates around the x- axis to show the labelled endothelial cells on the surface of non- stained cord tissue. Scale as in Figure 13.

Table 1

Primary Antibody	Minimum Effective Dilution	Positive Labelling in Tegu	Host	Source	Type
SV2	1:400	Synaptic vesicles, neurites at tegu neuromuscular junction	mouse	Developmental Studies Hybridoma Bank	monoclonal; multiple species
VAChT	1:400	Cholinergic vesicles, neurites at tegu neuromuscular junction; putative neurochemical cells lining carotid artery	Rabbit	Sigma V5387	polyclonal to an identified VAChT sequence; verified in mammals
5-HT	1: 100	Serotonin in adrenal cells; putative neurochemical cells lining carotid artery	Goat	Immunostar 20079	Polyclonal to serotonin; verified in mammals
5-HT	1:200	Serotonin in adrenal cells; putative neurochemical cells lining carotid artery	Rabbit	Sigma S5545	Polyclonal to serotonin; verified in mammals

Table 2

Secondary Antibody	Dilution used	Fluorescent conjugate	Excitation	Emission	Source
Donkey anti-mouse 594	1:400	Alexa 594	591	617	Invitrogen A21203
Donkey anti-goat 488	1:100	Alexa 488	488	519	Invitrogen A11055
Donkey anti-goat 568	1:100	Alexa 568	561	601	Invitrogen A11507
Donkey anti rabbit 488	1:100	Alexa 488	488	519	Invitrogen A21206
Donkey anti rabbit 594	1:100	Alexa 594	594	617	Invitrogen A21207

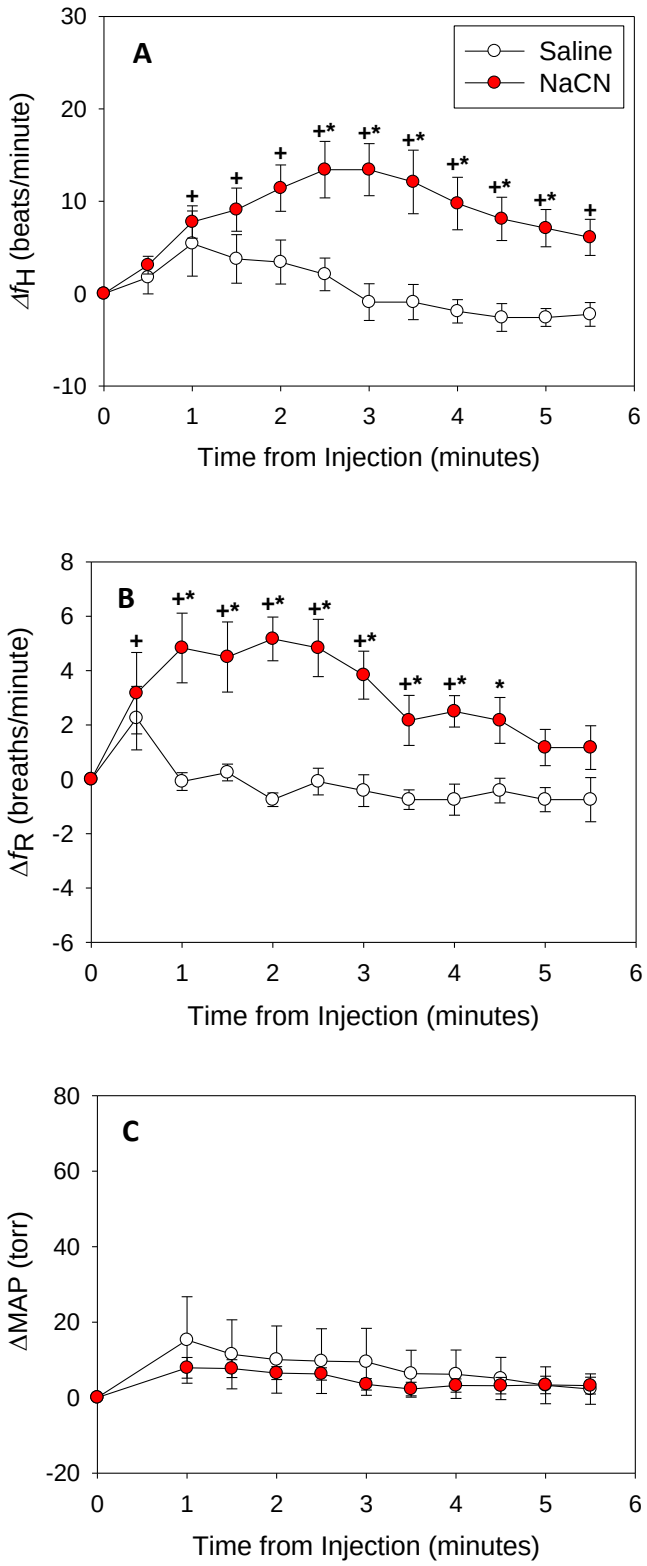

Figure 1

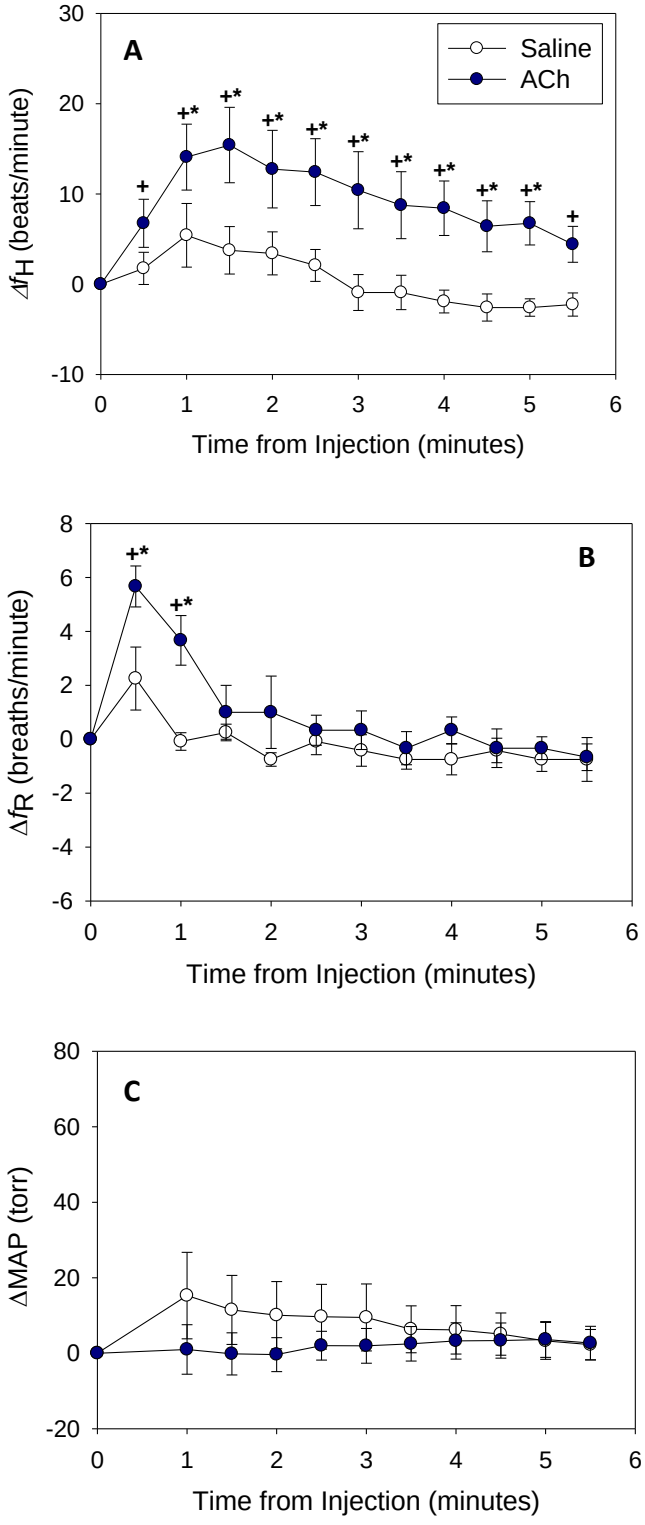

Figure 2

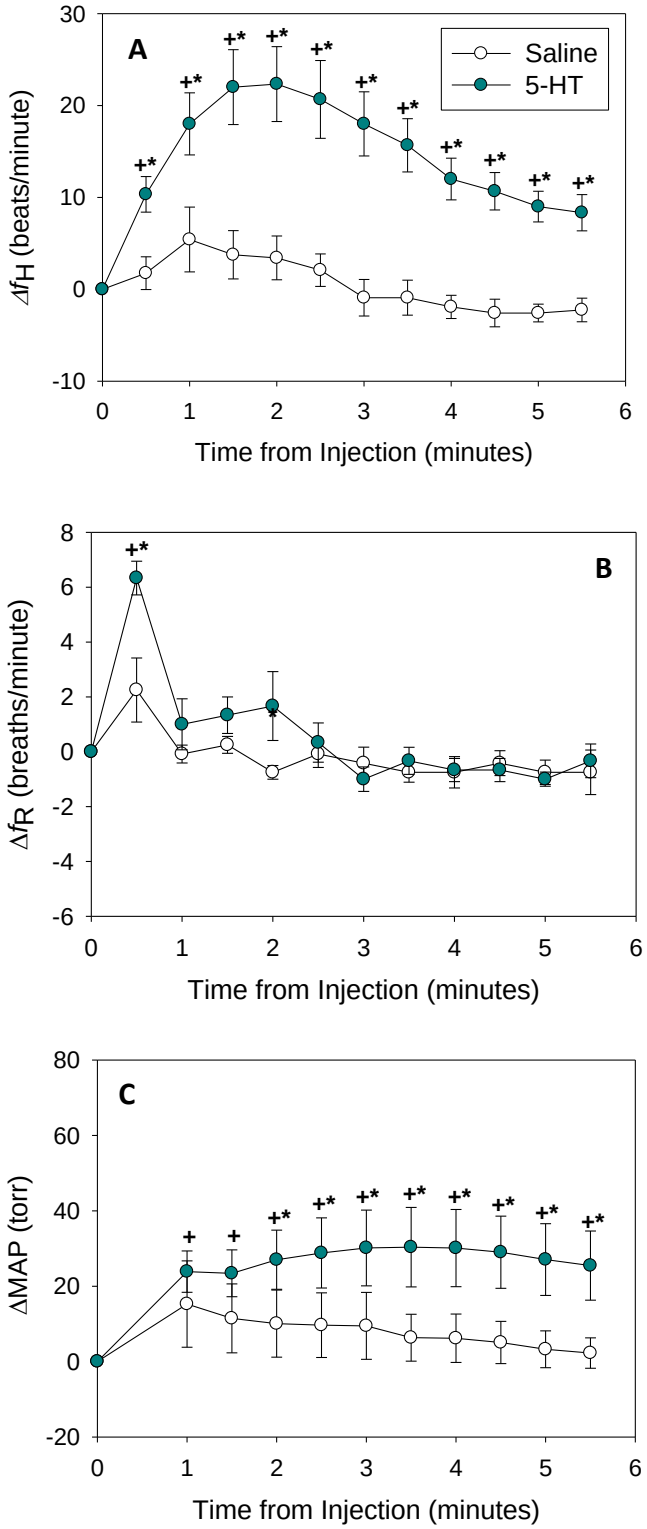

Figure 3

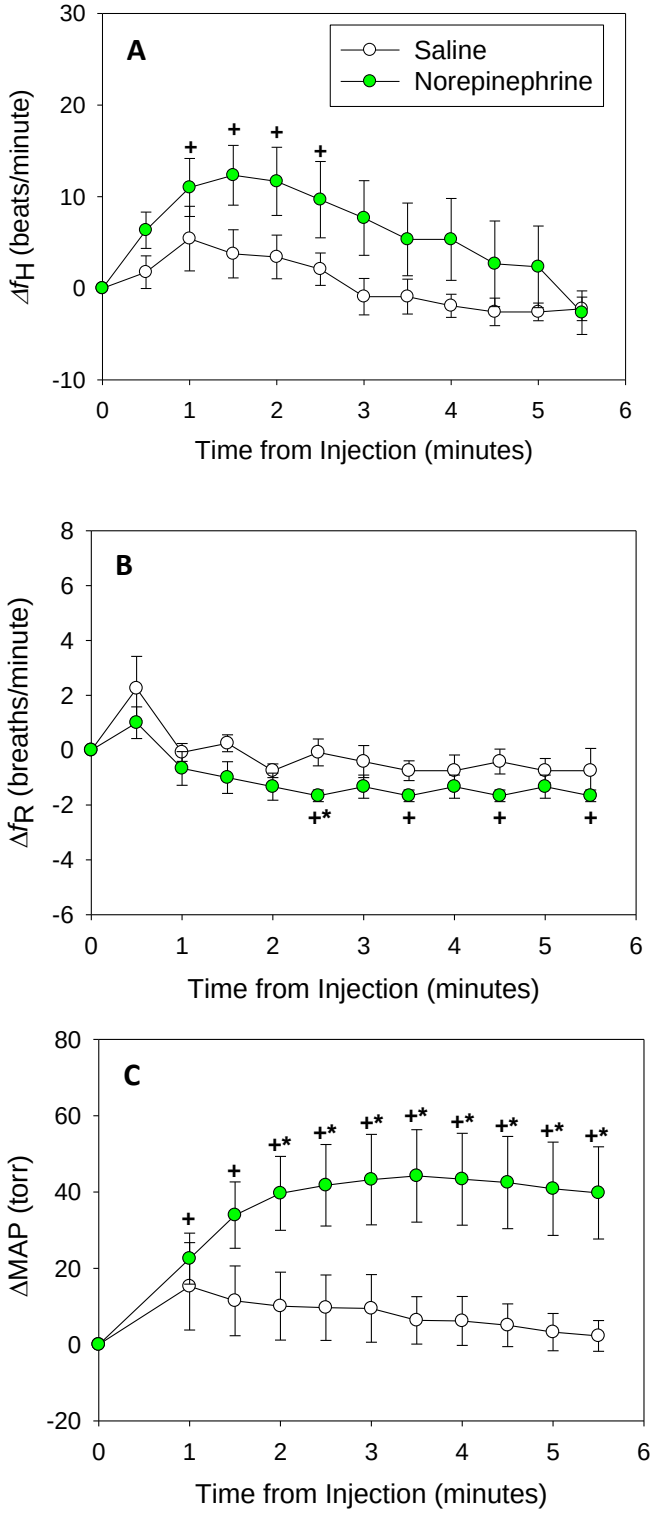

Figure 4

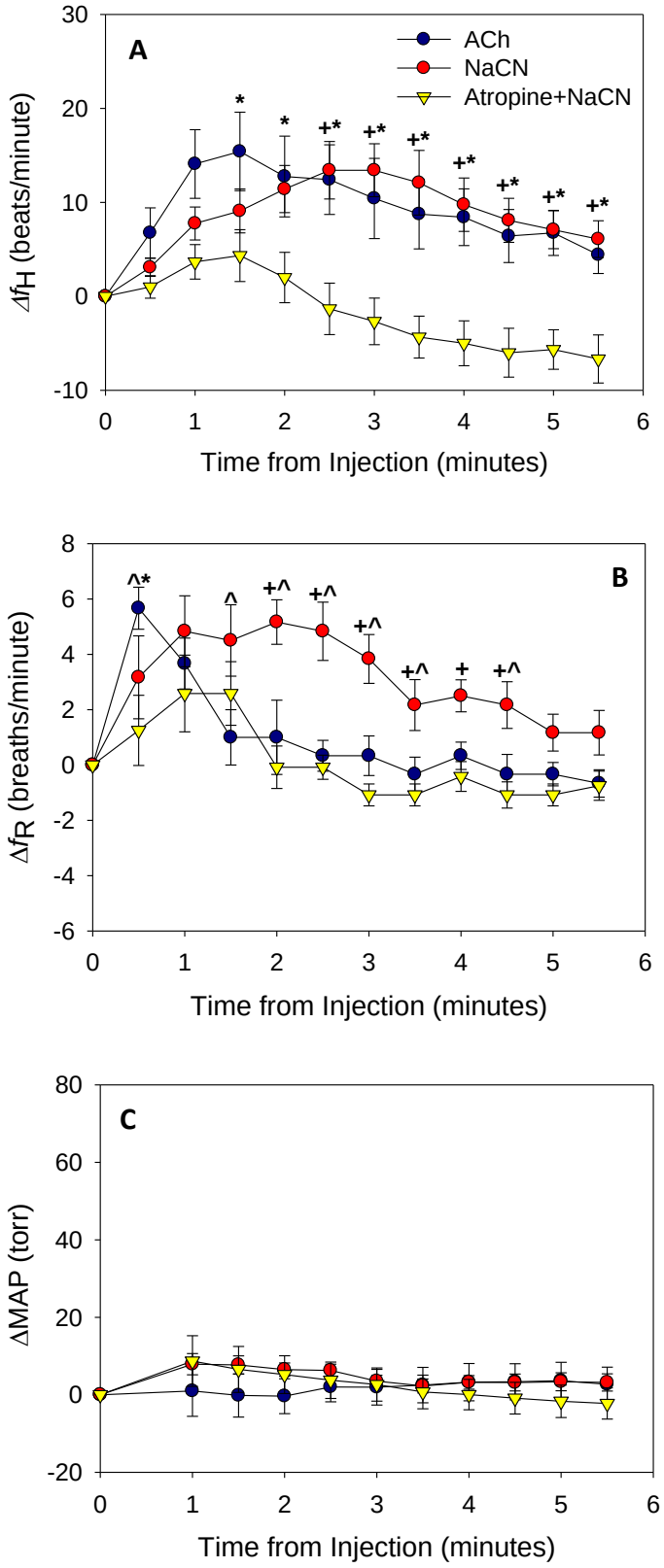

Figure 5

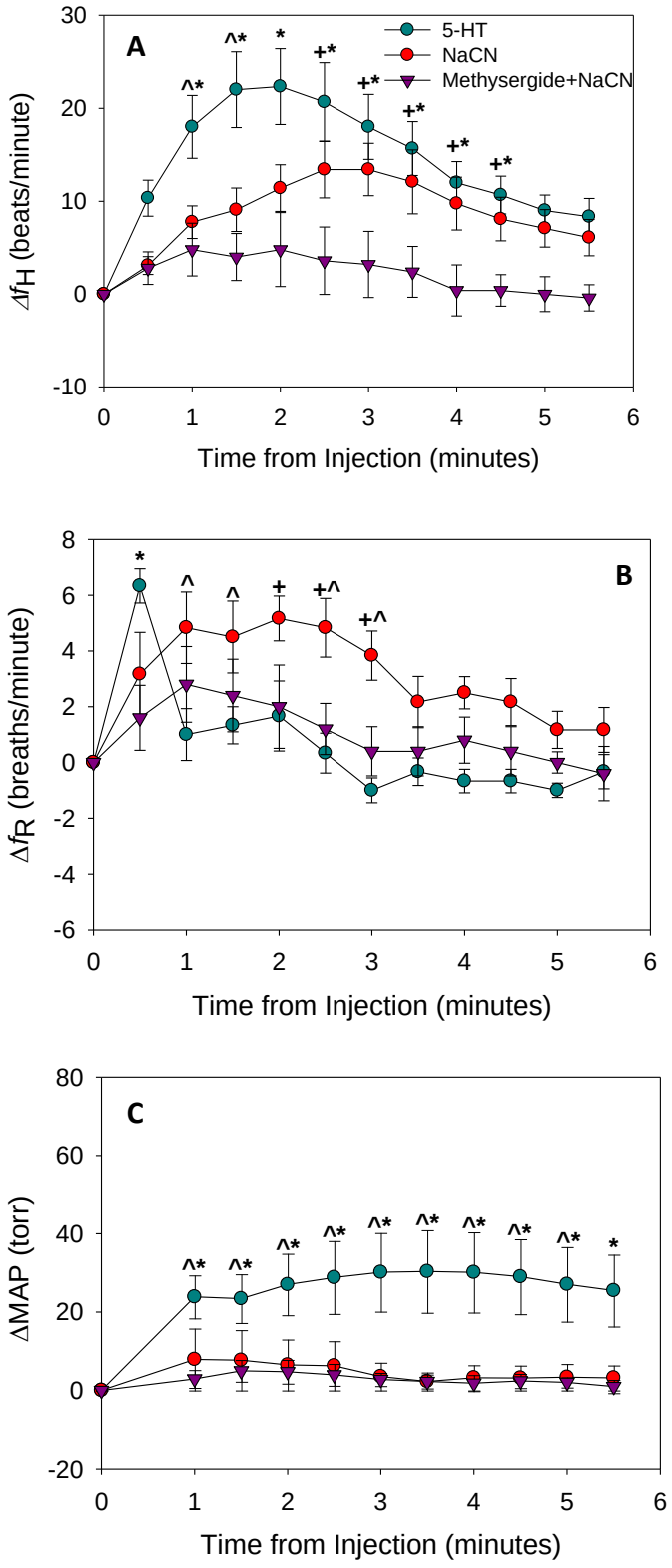

Figure 6

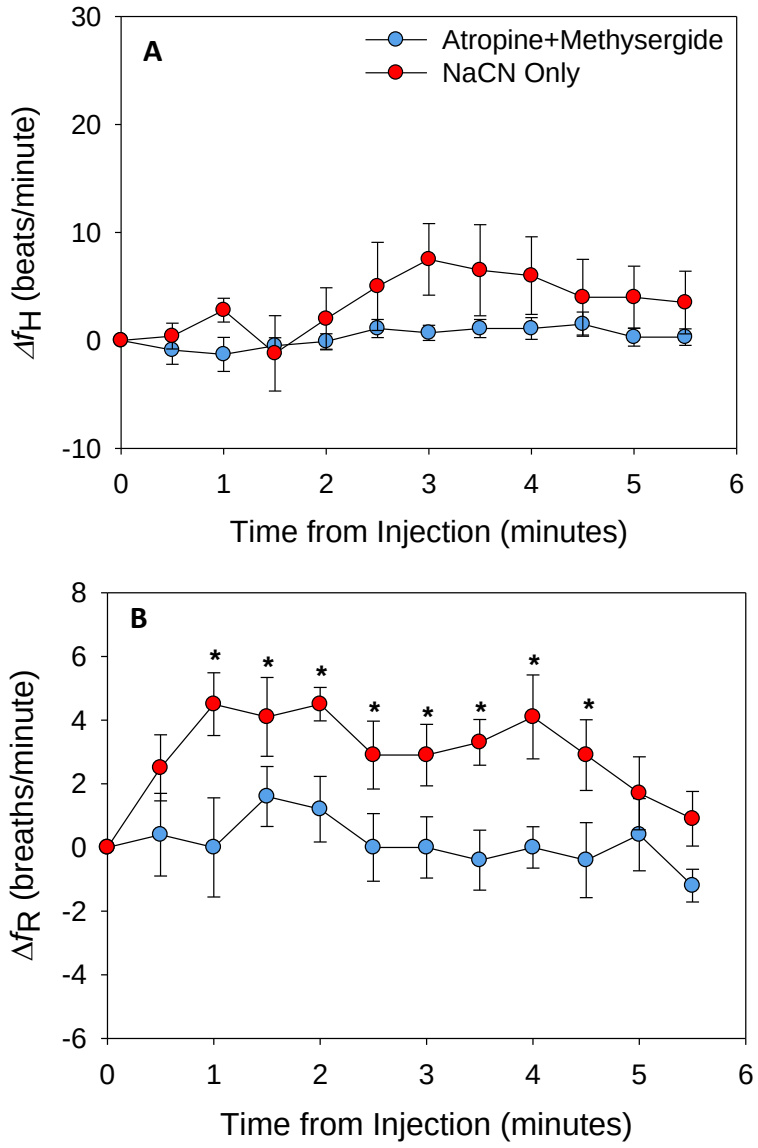

Figure 7

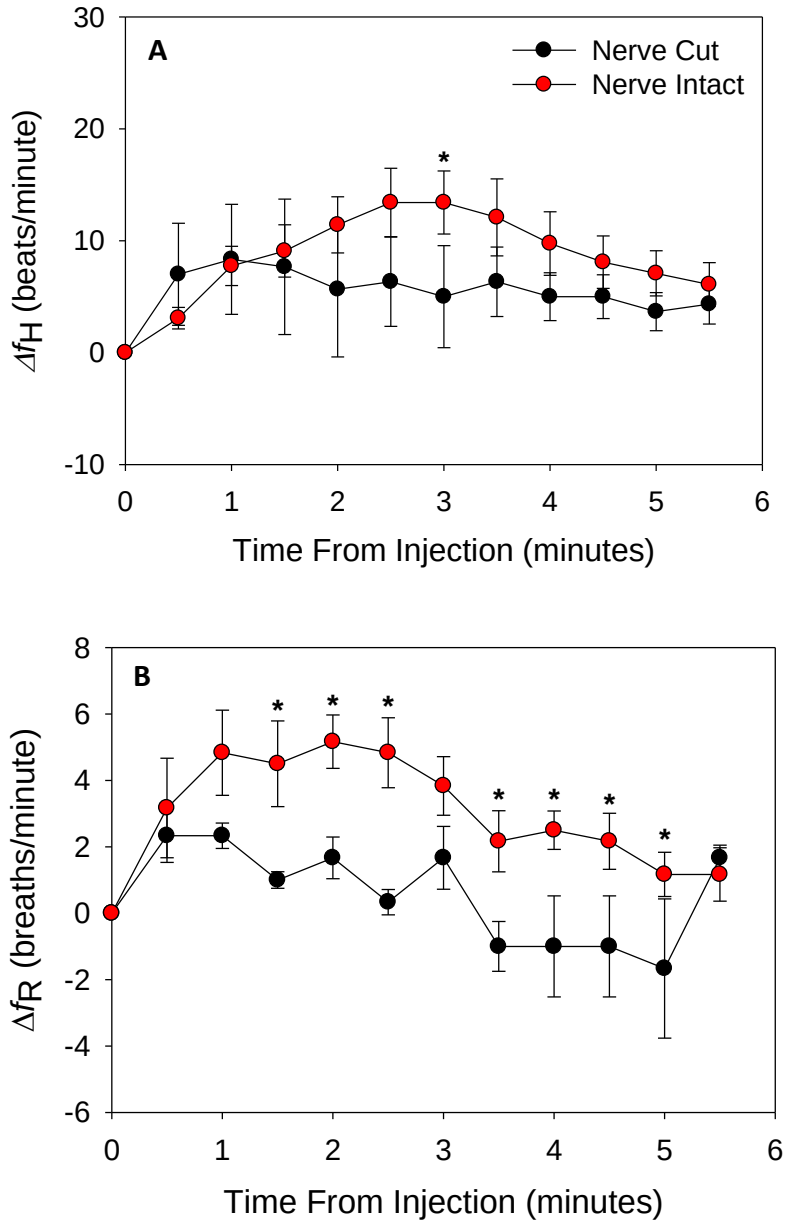

Figure 8

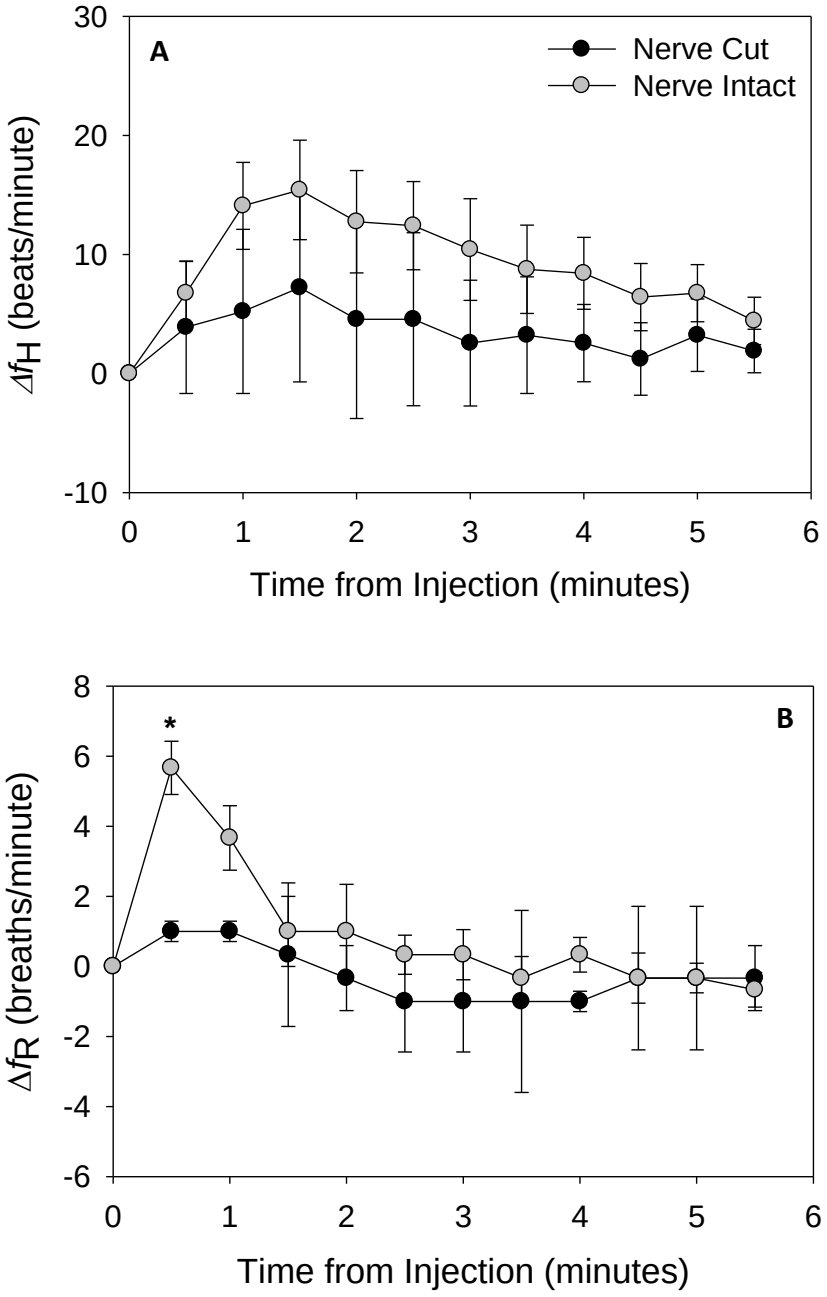

Figure 9

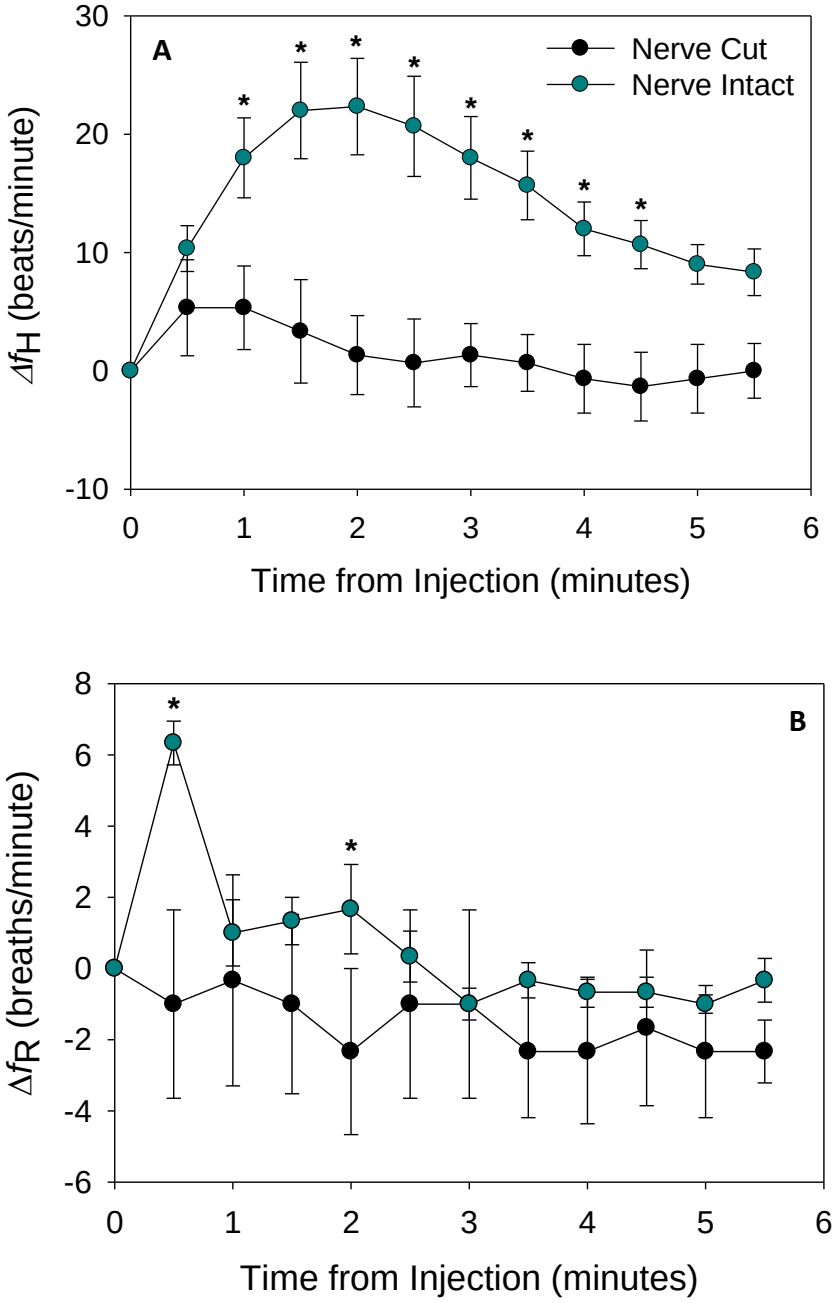

Figure 10

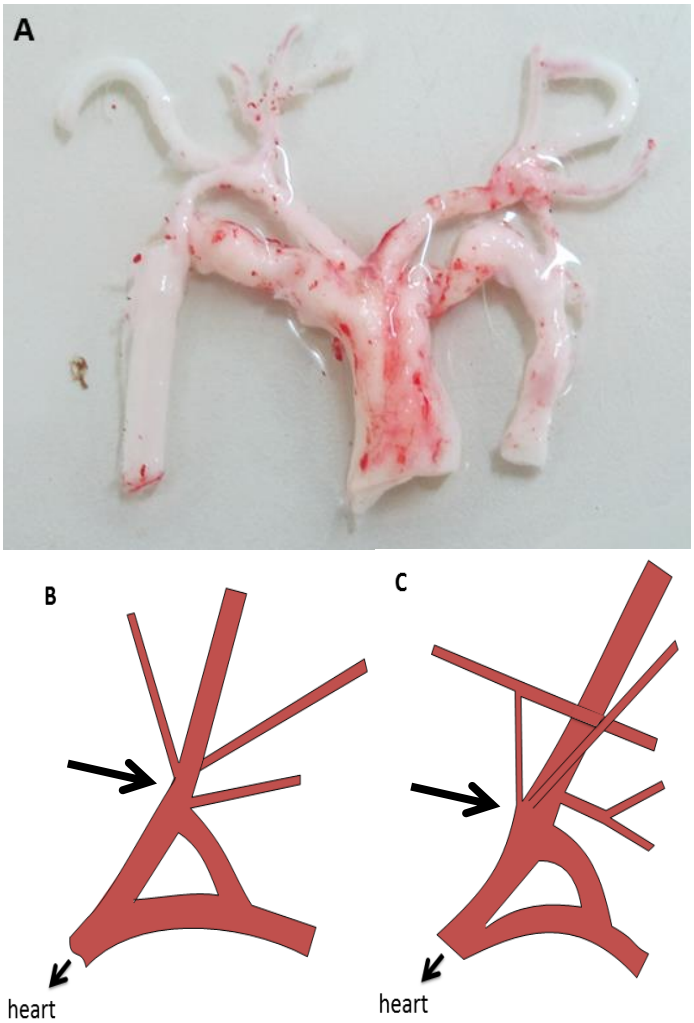

Figure 11

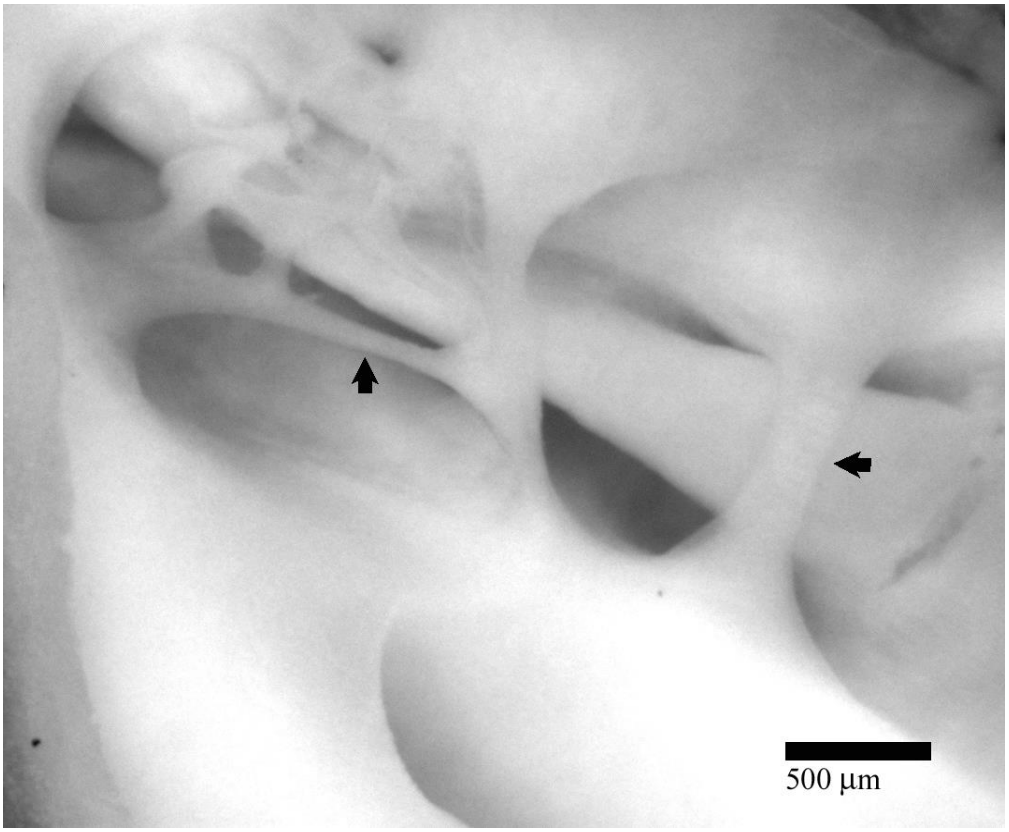

Figure 12

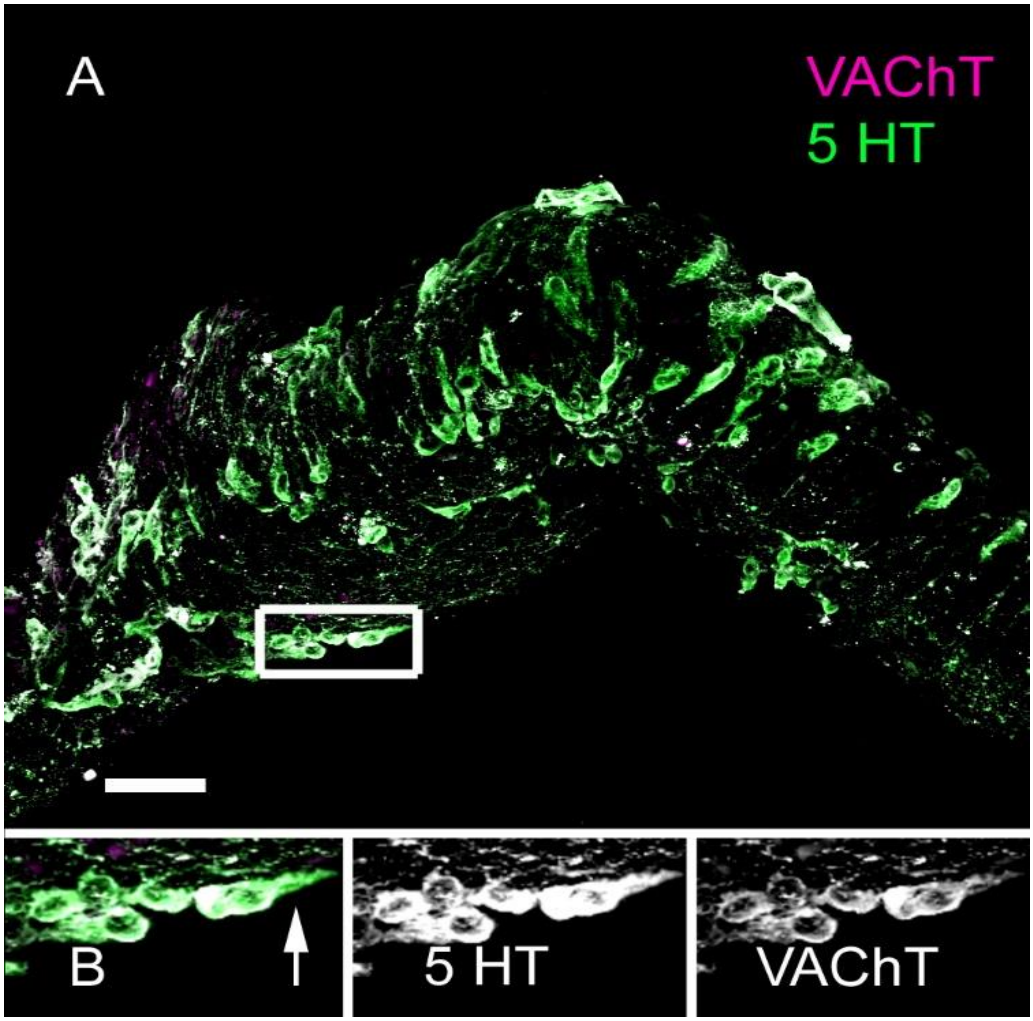

Figure 13